

# A theory of the strain-dependent critical field in Nb<sub>3</sub>Sn, based on anharmonic phonon generation

Davide Filippo Valentini,<sup>1,2</sup> Christophe Berthod,<sup>2</sup> Bernardo Bordini,<sup>1</sup> and Lucio Rossi<sup>1</sup>

<sup>1</sup>European Organization for Nuclear Research (CERN), 1211 Geneva 23, Switzerland

<sup>2</sup>Département de Physique de la Matière Condensée (DPMC),

University of Geneva, 24 quai Ernest-Ansermet, 1211 Geneva 4, Switzerland

(Dated: January 13, 2014)

We propose a theory to explain the strain dependence of the critical properties in A15 superconductors. Starting from the strong-coupling formula for the critical temperature, and assuming that the strain sensitivity stems mostly from the electron-phonon  $\alpha^2F$  function, we link the strain dependence of the critical properties to a widening of  $\alpha^2F$ . This widening is attributed to the nonlinear generation of phonons, which takes place in the anharmonic deformation potential induced by the strain. Based on the theory of sum- and difference-frequency wave generation in nonlinear media, we obtain an explicit connection between the widening of  $\alpha^2F$  and the anharmonic energy. The resulting model is fit to experimental datasets for Nb<sub>3</sub>Sn, and the anharmonic energy extracted from the fits is compared with first-principles calculations.

PACS numbers: 74.70.Ad, 74.25.Ld, 43.25.Dc

## I. INTRODUCTION

Nb<sub>3</sub>Sn is one of the prominent materials for present and future applications of superconductivity. It is used in high-field magnets for NMR spectroscopy,<sup>1</sup> for plasma confinement in nuclear fusion reactors,<sup>2</sup> in focusing and beam-steering magnets for particle accelerators, and is presently considered as a replacement for NbTi in the future upgrade of the Large Hadron Collider magnets.<sup>3</sup> Nb<sub>3</sub>Sn belongs to the crystalline symmetry group A15. It is a conventional superconductor with a critical temperature  $T_c$  around 17 K. The superconducting transition is well explained by the phonon-mediated pairing mechanism,<sup>4,5</sup> and the relatively high transition temperature can be understood in terms of a strong electron-phonon coupling, and a high density of states due to a narrow band of Nb 4d electrons at the Fermi energy.<sup>6</sup> The critical properties of Nb<sub>3</sub>Sn ( $T_c$ ,  $B_{c2}$ ,  $J_c$ ) vary considerably with the mechanical stress applied to the material. As the electromagnetic forces scale with the square of the fields, the strain dependence becomes increasingly important as the fields get higher. With a strong sensitivity to strain, Nb<sub>3</sub>Sn is an archetypical material to investigate and model the strain dependence of the critical surface in superconductors.

Previous investigations of the strain sensitivity of the critical parameters of Nb<sub>3</sub>Sn involved considerations associated with the structural transition from cubic to tetragonal symmetry.<sup>7</sup> The progressive refinement of empirical equations offered a description of uniaxial strain dependence,<sup>8,9</sup> as well as interpolation techniques for data analysis.<sup>10,11</sup> Following pioneering hints by Testardi,<sup>12</sup> the role of anharmonicity as a source of the strain dependence in Nb<sub>3</sub>Sn was later recognized and emphasized by Marckievicz.<sup>13</sup>

Here, we propose a microscopic mechanism to explain the effect of strain-induced anharmonicity on the phonon spectrum of Nb<sub>3</sub>Sn. A new scaling law for the strain dependence of the critical properties is deduced, based on the Migdal-Eliashberg strong-coupling theory of superconductivity. This

work has been triggered by recent studies,<sup>14</sup> showing that a relatively simple exponential expression of critical field and current dependence on strain [Eq. (19) of Ref. 14] is capable of well fitting experimental data of a large amount of samples, and over a large strain range.

The anharmonic terms in a crystalline potential induce interactions between phonons. In a quasi-particle description, these processes correspond to phonon-phonon scattering, and reduce the lifetime of the phonons. From a wavelike perspective, they can be regarded as energy and momentum exchange between coupled lattice vibrations. The latter conception, along with the general theory of resonance in nonlinear systems, offers a complementary insight: in a nonlinear medium, the mutual interaction of two coherent propagating waves generates new waves with sum and difference frequencies, at leading order in the nonlinearity. The new waves are amplified, and contribute to the total spectrum of excitations. Here we argue that the same mechanism can help understanding the effect of strain on phonons, and hence the detrimental effect of strain on superconductivity. The mechanical stress induces—or enhances—anharmonicity in the elastic potential. This favors the interaction between lattice waves, generating new waves with sum and difference frequencies. The phonon spectrum gets broadened, and the electron-phonon coupling is accordingly reduced, leading to a decrease of the critical properties.<sup>15</sup>

The simplest functional form which could describe the variation of the critical properties under strain, based on the conjecture that these variations are controlled by the strain-induced anharmonic energy  $\tilde{U}$ , is  $1/(1+A\tilde{U})$ , where  $A$  is a constant. Since  $\tilde{U}$  is an increasing function of strain, this formula yields a bell-shaped curve as a function of strain, consistently with experiments.<sup>14,16</sup> Our model yields the functional form  $1/\cosh[(B\tilde{U})^{1/2}]^\beta$ , with  $B$  a constant, and  $\beta$  a number of order one. Both forms agree at small  $\tilde{U}$ , provided  $A = \beta B/2$ , but the second form drops exponentially, rather than polynomially, at large  $\tilde{U}$ . An exponential dependence in the strain turns out to give a better description

of the available experimental datasets, as emphasized in Ref. 14.

The paper is organized as follows. The theory is presented in Sec. II, and its application to Nb<sub>3</sub>Sn in Sec. III. In Sec. II A, we briefly review the strong-coupling theory of superconductivity, emphasizing the role played by the width of the phonon density of states. Section II B deals with the effect of anharmonicity on the phonon spectrum. The strain function and the resulting model for the critical field are presented in Sec. II C. In Sec. III, we first discuss the strain state in Nb<sub>3</sub>Sn wires, and propose a parametrization of the anharmonic energy (Sec. III A). We then present fits of the model to experimental data, and compare the extracted anharmonic energy with first-principles calculations (Sec. III B). Our conclusions and perspectives are summarized in Sec. IV. Appendices A and B contain general considerations about nonlinear elasticity, our first-principles calculations of the Nb<sub>3</sub>Sn elastic constants, and a discussion of the nonlinear generation of acoustic waves.

## II. THEORY

### A. Strong-coupling superconductivity and strain-dependent critical temperature

The strong-coupling theory of superconductivity extends the Bardeen-Cooper-Schrieffer theory by including the dynamical structure of the phonon-mediated pairing, in particular the retardation effects.<sup>17</sup> The main ingredient of the theory is the electron-phonon spectral function  $\alpha^2F(\omega)$ , which gives an average of the square of the electron-phonon matrix element for electrons on the Fermi surface exchanging phonons of frequency  $\omega$ . The numerical solution of the strong-coupling equations for the critical temperature  $T_c$  has been cast in a simple analytical formula,<sup>18–20</sup> which depends on a small number of physically meaningful parameters:

$$k_B T_c = \frac{\hbar \langle \omega \rangle}{1.20} \exp \left[ -\frac{1.04(1 + \lambda)}{\lambda - \mu^*(1 + 0.62\lambda)} \right]. \quad (1)$$

Here,  $\langle \omega \rangle$  is of the order of the average phonon frequency,  $\mu^*$  gives the strength of the screened Coulomb repulsion on the Fermi surface,<sup>21</sup> and  $\lambda$  is a dimensionless parameter measuring the strength of the electron-phonon interaction. The latter is related to the  $\alpha^2F$  function by

$$\lambda = 2 \int_0^\infty d\omega \frac{\alpha^2F(\omega)}{\omega}. \quad (2)$$

This parameter also determines the renormalization of the Fermi velocity  $v_F^* = v_F/(1 + \lambda)$  by the electron-phonon interaction, as well as the enhancement of the electronic specific heat coefficient  $\gamma = (1 + \lambda)\gamma_0$  with respect to the band value. Alternatively, the coupling  $\lambda$  may be written as<sup>18</sup>

$$\lambda = \frac{N(E_F) \langle \mathcal{G}^2 \rangle}{M \langle \omega^2 \rangle}, \quad (3)$$

where  $N(E_F)$  is the electronic density of states (DOS) at the Fermi level,  $\langle \mathcal{G}^2 \rangle$  is the electronic contribution to the Fermi-surface average of the squared electron-phonon matrix element, and  $M$  is the average ionic mass. The remaining parameter in Eq. (3),  $\langle \omega^2 \rangle$ , will be our main concern. It is defined as

$$\langle \omega^2 \rangle = \frac{2}{\lambda} \int_0^\infty d\omega \omega \alpha^2F(\omega). \quad (4)$$

For a single Einstein phonon of frequency  $\omega_0$ , we have  $\langle \omega^2 \rangle = \omega_0^2$ . For a Debye spectrum, assuming that  $\alpha^2F$  is simply proportional to the quadratic phonon DOS, we find  $\langle \omega^2 \rangle = \omega_D^2/2$ , where  $\omega_D$  is the Debye frequency. Thus, for a general phonon spectrum,  $\langle \omega^2 \rangle^{1/2}$  gives a measure of the width of the phonon DOS.

The central assumption of the present study is that the strain-induced variation of the critical properties in Nb<sub>3</sub>Sn and similar compounds is dominated by changes in the phonon spectrum. We accordingly infer that the purely electronic quantities, namely  $\mu^*$ ,  $N(E_F)$ , and  $\langle \mathcal{G}^2 \rangle$  in Eqs. (1) and (3), can be considered strain-independent in a first approximation. Recent first-principles calculations for Nb<sub>3</sub>Sn suggest that the electron and phonon spectra both vary with the applied strain.<sup>22</sup> So far, however, the question whether the strain sensitivity in A15 superconductors is due mainly to lattice or to electronic degrees of freedom has not been settled, neither experimentally nor theoretically.<sup>9,23,24</sup> The justification for the present approach comes primarily from its ability to describe experimental data.

We propose that the interactions between phonons, generated by the anharmonic terms in the elastic energy, produce secondary vibrational modes with sum and difference frequencies, as discussed in more detail in the next section. This process leads to a broadening of the phonon spectrum, hence to an increase of  $\langle \omega^2 \rangle$ . A change in  $\langle \omega \rangle$  may also result, but this change is expected to be small compared with the change of  $\langle \omega^2 \rangle$ , due to cancellations between sum and difference frequencies. Moreover, since  $\langle \omega^2 \rangle$  goes into the exponential in the formula (1), while  $\langle \omega \rangle$  enters only as a pre-factor, we will neglect the variation of  $\langle \omega \rangle$  hereafter for simplicity. Another simplification arises, because the value of the screened Coulomb repulsion is generally small with respect to  $\lambda$  in A15 compounds. A few representative values are listed in Table I. Neglecting terms of order  $\mu^*/\lambda$  in the square brackets in Eq. (1), we form the ratio between the critical temperature  $T_c(\varepsilon)$  in the presence of

TABLE I. Electron-phonon coupling  $\lambda$ , and screened Coulomb repulsion  $\mu^*$ , for some A15 superconductors.

Material	$\lambda$	$\mu^*$	Ref.
Nb <sub>3</sub> Sn	1.80	0.16	25
Nb <sub>3</sub> Al	1.70	0.15	26
Nb <sub>3</sub> Ge	1.64	0.12	27 <sup>a</sup>
V <sub>3</sub> Si	1.07	0.13	28

<sup>a</sup> Values for the sample with the highest  $T_c$

a strain described by the tensor  $\boldsymbol{\varepsilon}$ , and the value  $T_c(0)$  at equilibrium:

$$\frac{T_c(\boldsymbol{\varepsilon})}{T_c(0)} = \exp \left[ -\frac{1.04}{\lambda(0)} \left( \frac{\lambda(0)}{\lambda(\boldsymbol{\varepsilon})} - 1 \right) \right]. \quad (5)$$

Considering Eq. (3), we furthermore see that  $\lambda(0)/\lambda(\boldsymbol{\varepsilon}) = \langle \omega_\varepsilon^2 \rangle / \langle \omega_0^2 \rangle$ , where  $\langle \omega_0^2 \rangle$  (respectively,  $\langle \omega_\varepsilon^2 \rangle$ ) is the value of the parameter  $\langle \omega^2 \rangle$  at equilibrium (respectively, under strain). We conclude that, according to the hypotheses made so far, the strain-induced variation of  $T_c$  depends on the relative variation of the phonon-spectrum “width”, more precisely the parameter  $\langle \omega^2 \rangle$ .

### B. Broadening of the phonon spectrum by nonlinear wave generation

As stated in the Introduction, the interaction between phonons can be viewed, in a quasi-particle picture, as phonon-phonon scattering processes, which reduce the lifetime and the mean-free path of the phonons. Alternatively, it may be regarded as the generation of secondary waves in a nonlinear medium. In both views, the interaction has the effect of widening the phonon spectrum of a hypothetical perfect harmonic crystal, either by broadening individual phonon lines in the former view, or by adding additional phonon modes in the latter—which is the preferred view in the present study. Phonon-phonon interactions are present in materials even at equilibrium, due to intrinsic anharmonic terms in the elastic deformation potential. The application of a stress, with the associated deformation of the unit cell, reinforces anharmonic contributions by driving the crystal away from its equilibrium point. The width of the electron-phonon spectral function  $\alpha^2 F(\omega)$ , and consequently the parameter  $\langle \omega^2 \rangle$ , are expected to increase with the applied strain, reflecting the increased interaction among phonons. We may introduce two limiting values,  $\langle \omega_0^2 \rangle$  and  $\langle \omega_1^2 \rangle$ , corresponding respectively to the equilibrium state, and to a high-strain state where the generation of secondary phonons with sum and difference frequencies would have exhausted all pairs of primary phonons. Between these two limits, we parametrize the variation of  $\langle \omega^2 \rangle$  with strain as

$$\langle \omega_\varepsilon^2 \rangle - \langle \omega_0^2 \rangle = w(\boldsymbol{\varepsilon}) \left( \langle \omega_1^2 \rangle - \langle \omega_0^2 \rangle \right), \quad (6)$$

where, by assumption, the anharmonic weight factor  $w(\boldsymbol{\varepsilon})$  is proportional to the total amplitude of the secondary waves generated by the strain-induced anharmonic terms in the elastic energy.

In order to build a model for  $w(\boldsymbol{\varepsilon})$ , we borrow idea familiar in nonlinear optics.<sup>29</sup> Two electromagnetic waves with frequencies  $\omega_1$  and  $\omega_2$ , entering a nonlinear resonant cavity, generate secondary waves with frequencies  $\omega_3 = \omega_1 \pm \omega_2$ , at first order in the nonlinearity. The wave generation obeys energy conservation rules, and phase matching conditions for the momenta.<sup>29</sup> The amplitudes of the primary waves progressively die out, while their energy is transferred to the secondary waves, whose amplitudes grow. A

very similar phenomenon occurs for acoustic waves in a nonlinear elastic medium. The case of longitudinal waves is presented in Appendix B. We find that the amplitude  $A_3$  of the secondary waves increase in time according to  $\omega_3 A_3(t) = (\tilde{U}/\rho)^{1/2} \tanh[tq_{12}(\tilde{U}/\rho)^{1/2}]$ , where  $\tilde{U}$  is the energy transferred from the primary to the secondary waves,  $\rho$  is the mass density of the medium, and  $q_{12} = |b/2|/\sqrt{q_1 q_2}$ , with  $b$  a nonlinear factor [Eq. (A4)], and  $q_{1,2}$  the wave numbers of the primary waves. If the primary waves interact coherently with a negligible damping during a time  $\tau$ , the total amplitude generated during the coherence time is therefore

$$\int_0^\tau dt A_3(t) \propto \ln \left[ \cosh \left( \sqrt{\tilde{U}/\rho} q_{12} \tau \right) \right], \quad (7)$$

where the pre-factor is independent of the energy  $\tilde{U}$ . As the weight factor  $w(\boldsymbol{\varepsilon})$  should be dimensionless, and proportional to the amplitude of generated waves, it is natural to take

$$w(\boldsymbol{\varepsilon}) = \ln \left[ \cosh \left( \sqrt{\tilde{U}(\boldsymbol{\varepsilon})/\rho} Q \tau \right) \right]. \quad (8)$$

$\tilde{U}(\boldsymbol{\varepsilon})$  is the strain-induced anharmonic energy available for the generation of secondary phonons, and  $Q = |b/2|/\sqrt{q_1 q_2}$  is a typical phonon momentum. Considering that the primary momenta  $q_{1,2}$  vary between 0 and  $\omega_D/v$ , with  $v$  the velocity of sound, we find in three dimensions  $\langle \sqrt{q_1 q_2} \rangle = (36/49)\omega_D/v \approx (3/4)\omega_D/v$ . Finally,  $\tau$  plays the role of a phonon coherence time. At low temperature, it is given by the average phonon lifetime, while at high temperature it is cut by the thermal limit  $h/(k_B T)$ . Equation (8) correctly gives  $w(0) = 0$ , as well as  $w(\boldsymbol{\varepsilon}) \equiv 0$  in the absence of anharmonicity ( $b = 0$ ).

### C. Exponential strain function and critical field

The set of equations (8), (6), (5), and (3) lead, after a simple algebra, to the expression

$$\frac{T_c(\boldsymbol{\varepsilon})}{T_c(0)} = \cosh \left( \sqrt{\tilde{U}(\boldsymbol{\varepsilon})/\rho} Q \tau \right)^{-\frac{1.04}{\lambda(0)} \left( \frac{\langle \omega_\varepsilon^2 \rangle}{\langle \omega_0^2 \rangle} - 1 \right)}. \quad (9)$$

As the exponent is negative, and  $\tilde{U}(\boldsymbol{\varepsilon})$  is expected to increase monotonically with increasing strain,  $T_c(\boldsymbol{\varepsilon})$  is expected to be a monotonically decreasing function of strain according to Eq. (9). It is customary to introduce a “strain function”  $s(\boldsymbol{\varepsilon})$  in order to describes the strain dependence of the upper critical field at zero temperature:

$$s(\boldsymbol{\varepsilon}) = \frac{B_{c2}(\boldsymbol{\varepsilon})}{B_{c2}(0)}. \quad (10)$$

Experimentally, it was found<sup>8</sup> that the strain dependence of  $T_c$  scales with that of  $B_{c2}$ , i.e.,  $T_c(\boldsymbol{\varepsilon})/T_c(0) = [B_{c2}(\boldsymbol{\varepsilon})/B_{c2}(0)]^{1/\alpha}$  with  $\alpha \approx 3$ . This leads to the following model for the strain function:

$$s(\boldsymbol{\varepsilon}) = \cosh \left( \sqrt{\tilde{U}(\boldsymbol{\varepsilon})/\rho} Q \tau \right)^{-\frac{1.04\alpha}{\lambda(0)} \left( \frac{\langle \omega_\varepsilon^2 \rangle}{\langle \omega_0^2 \rangle} - 1 \right)}. \quad (11)$$

Equation (11) is our main result. It shows that the strain dependence of  $s(\boldsymbol{\varepsilon})$  stems from the strain-induced anharmonic contributions to the elastic energy. The temperature dependence of the critical field is described by the scaling law<sup>30</sup>  $B_{c2}(T)/B_{c2}(0) = (1 - T/T_c)^\gamma$ , with an exponent  $\gamma \approx 1.5$ . We can therefore write the temperature- and strain-dependent critical field in the form

$$B_{c2}(T, \boldsymbol{\varepsilon}) = B_{c20} \left\{ 1 - \left( \frac{T}{T_{c0}} \right)^\gamma [s(\boldsymbol{\varepsilon})]^{-\frac{\gamma}{\alpha}} \right\} s(\boldsymbol{\varepsilon}), \quad (12)$$

where  $B_{c20}$  is the zero-temperature and zero-strain upper critical field, and  $T_{c0}$  is the zero-strain critical temperature. In the next section, we use Eqs. (11) and (12) to fit critical-field data measured on Nb<sub>3</sub>Sn wires, extract the anharmonic energy  $\tilde{U}(\boldsymbol{\varepsilon})$ , and compare with the anharmonic energy calculated from first principles for bulk Nb<sub>3</sub>Sn strained like in the wires.

### III. APPLICATION TO Nb<sub>3</sub>SN SUPERCONDUCTING WIRES

#### A. Anharmonic energy of pre-strained Nb<sub>3</sub>Sn

In order to compare the model (11) and (12) with experimental determinations of  $B_{c2}(T, \boldsymbol{\varepsilon})$ , we have to specify the strain, and to parametrize the behavior of  $\tilde{U}(\boldsymbol{\varepsilon})$ . Following Ref. 31, we introduce three invariants  $I_1$ ,  $J_2$ , and  $J_3$  to represent the deformation.  $I_1$  is the hydrostatic invariant, given by  $I_1 = \varepsilon_1 + \varepsilon_2 + \varepsilon_3$ , where  $\varepsilon_i$  are the values of the strain along the three principal directions.  $J_2$  and  $J_3$  are the second and third deviatoric invariants, defined as  $J_2 = [(\varepsilon_1 - \varepsilon_2)^2 + (\varepsilon_2 - \varepsilon_3)^2 + (\varepsilon_3 - \varepsilon_1)^2]/6$ , and  $J_3 = (\varepsilon_1 - I_1/3)(\varepsilon_2 - I_1/3)(\varepsilon_3 - I_1/3)$ . In a harmonic crystal, the elastic energy is quadratic, and takes a simple form in terms of the two second-order invariants  $I_1^2$  and  $J_2$ ,

$$U_{\text{harm}} = \frac{1}{6} \frac{E}{1 - 2\nu} I_1^2 + \frac{E}{1 + \nu} J_2, \quad (13)$$

where  $E$  is the Young modulus and  $\nu$  is the Poisson ratio (see Appendix A). This harmonic energy does not contribute to the interaction between phonons. Under the effect of stress, additional terms of higher orders in the strain contribute to the elastic energy. Terms of third order can be proportional to  $I_1^3$ ,  $I_1 J_2$ , and  $J_3$ , while terms of fourth order include the combinations  $I_1^4$ ,  $I_1^2 J_2$ ,  $I_1 J_3$ , and  $J_2^2$ . Our goal is to represent the anharmonic energy—an increasing function of strain—with as few parameters as possible. We therefore exclude contributions which are not positive-definite as a function of strain. With the strain configuration of interest to us, namely  $\varepsilon_2 = \varepsilon_3$  (see below), this excludes all third-order terms, as well as the fourth-order term  $I_1 J_3$ : all of them are odd functions of  $\varepsilon_1 + 2\varepsilon_2$  and/or  $\varepsilon_1 - \varepsilon_2$ . Our parametrization of the anharmonic energy is therefore

$$\tilde{U}(\boldsymbol{\varepsilon}) = p_1 I_1^4 + p_{12} I_1^2 J_2 + p_2 J_2^2. \quad (14)$$

The three parameters are nonnegative, and have the unit of energy per unit volume, i.e., pressure. One further con-

straint will emerge from the analysis of our particular strain model.

Here we focus on the strain experienced by Nb<sub>3</sub>Sn strands during critical-current measurements under applied longitudinal strain. In order to describe these strain conditions, we use the same assumptions as in Ref. 14: the principal strain component  $\varepsilon_1$  is along the strand axis;  $\varepsilon_1 = \varepsilon_{l0} + \varepsilon_a$ ;  $\varepsilon_2 = \varepsilon_3 = \varepsilon_{t0} - \nu \varepsilon_a$ , where  $\varepsilon_{l0}$  and  $\varepsilon_{t0}$  are the initial longitudinal and transverse strains, respectively, and  $\nu$  is the effective poisson ratio, for which we use the value  $\nu = 0.36$  as in Ref. 14. Rewriting the pre-strain as the sum of an hydrostatic part  $\varepsilon_0$ , and a deviatoric part  $\varepsilon_{10}$ , these relations become  $\varepsilon_1 = \varepsilon_0 + \varepsilon_{10} + \varepsilon_a$ , and  $\varepsilon_2 = \varepsilon_3 = \varepsilon_0 - \nu \varepsilon_{10} - \nu \varepsilon_a$ .

Upon varying  $\varepsilon_a$ , the critical field goes through a maximum at a strain close to the value  $\varepsilon_a^*$ , which restores the cubic symmetry of the superconductor.<sup>10,32</sup> In the strain configuration described above, we have  $\varepsilon_a^* = -\varepsilon_{10}$ , which implies  $I_1(\varepsilon_a^*) = 3\varepsilon_0$ , and  $J_2(\varepsilon_a^*) = 0$ . Therefore, the anharmonic energy  $\tilde{U}(\varepsilon_a^*) = p_1(3\varepsilon_0)^4$  accounts for the reduction of the critical field under purely hydrostatic strain. The consistency of the model requires that the function  $\tilde{U}(\boldsymbol{\varepsilon})$  as a function of  $\varepsilon_a$  has a single minimum close to  $\varepsilon_a = \varepsilon_a^*$ , and otherwise varies monotonically. By constraining the parameters to satisfy  $p_2/p_{12} > \theta(1 - 4\theta p_1/p_{12})/(1 + 12\theta p_1/p_{12})$ , with  $\theta = (3/2)[(1 - 2\nu)/(1 + \nu)]^2$ , we ensure that the second derivative of  $\tilde{U}(\boldsymbol{\varepsilon})$  with respect to  $\varepsilon_a$  is positive for any strain.

Before turning to the fits, we note that the parametrization (14) may not be the best choice in every situation. In the case of pre-strained wires, the formula (14) generates all powers of  $\varepsilon_a$  from zero to four, and has enough freedom to grant a good fit. For hydrostatic pressure, however, Eq. (14) only contains the fourth power of the strain. In this case, it may prove necessary to retain a term proportional to  $I_1^3$ .

#### B. Fits to critical-field data, and discussion of the anharmonic energy

With the parametrization (14), and enforcing the inequality on  $p_2/p_{12}$ , the strain function (11) can be recast in the form

$$s(\boldsymbol{\varepsilon}) = \left[ \cosh \left( C_0 \sqrt{C_1 I_1^4 + I_1^2 J_2 + (\delta + C_2) J_2^2} \right) \right]^{-\beta} \quad (15a)$$

$$I_1 = (1 - 2\nu)(\varepsilon_a - \varepsilon_a^*) + 3\varepsilon_0 \quad (15b)$$

$$J_2 = (1/3)(1 + \nu)^2 (\varepsilon_a - \varepsilon_a^*)^2 \quad (15c)$$

$$\delta = \theta(1 - 4\theta C_1)/(1 + 12\theta C_1) \quad (15d)$$

$$\theta = (3/2)[(1 - 2\nu)/(1 + \nu)]^2. \quad (15e)$$

The positive dimensionless parameters  $C_0$ ,  $C_1$ , and  $C_2$  are related to the parameters giving the anharmonic energy (14) by  $p_{12} = \rho [C_0/(Q\tau)]^2$ ,  $p_1 = C_1 p_{12}$ , and  $p_2 = (\delta + C_2) p_{12}$ . The exponent  $\beta$  depends on the electron-phonon coupling  $\lambda(0)$ , and on the broadening of the phonon spectrum  $\langle \omega_1^2 \rangle / \langle \omega_0^2 \rangle$ , as can be seen from Eq. (11). An estimate of this exponent for Nb<sub>3</sub>Sn may be obtained as

follows. The  $\alpha^2 F$  function determined by inverting tunneling data in Ref. 33 has four main features, at 4.5, 8.0, 18.6, and 24.9 meV. A very crude way of computing  $\langle \omega_0^2 \rangle$  is to use  $\langle \omega_0^2 \rangle \approx (\sum_i \omega_i) / (\sum_i \omega_i^{-1})$ , where the sums run over the four characteristic frequencies. The result is  $\langle \omega_0^2 \rangle^{1/2} \approx 11.3$  meV. In order to check the reliability of this approximation, we take the complete  $\alpha^2 F$  function from Ref. 33, and perform the integrals in Eqs. (2) and (4). This gives the values  $\lambda = 2.74$  and  $\langle \omega^2 \rangle^{1/2} = 12.6$  meV. The latter exact value is quite close to the approximate result 11.3 meV. This suggests to compute  $\langle \omega_1^2 \rangle$  by the same method: from the set of characteristic frequencies, we build the set of sum and difference frequencies, which together give  $\langle \omega_1^2 \rangle^{1/2} \approx 15.8$  meV. Using  $\alpha = 3$  and  $\lambda(0) = 2.74$ , we finally deduce  $\beta = 1.09$ .

The behavior of  $s(\epsilon)$  close to the point  $\epsilon_a^*$  may be studied by expanding Eq. (15) as  $s(\epsilon) = 1 / [1 + \sum_i a_i (\epsilon_a - \epsilon_a^*)^i]$ . The zeroth order coefficient is  $a_0 = (81/2)\beta C_0^2 C_1 \epsilon_0^4$ , to leading order in  $\epsilon_0$ . This confirms that, according to the model (15), the critical field decreases as  $\epsilon_0^4$  under hydrostatic strain. Up to fourth order, the coefficients  $a_i$  involve the combinations  $\beta C_0^2$ ,  $\beta C_0^2 C_1$ , and  $\beta C_0^2 C_2$ . Therefore, only three of the four parameters  $\beta, C_{0,1,2}$  can be determined by fitting experimental data close to  $\epsilon_a = \epsilon_a^*$ : variations of the parameter  $\beta$  can be absorbed into a redefinition of  $C_0$ . In view of this, we shall adopt the value  $\beta = 1$  in the following, when fitting (12) and (15) to experimental data.

Fitting the model to the Furukawa dataset of Ref. 14, we find that  $C_2 = 0$ , which implies that the inequality imposed on  $p_2/p_{12}$  is saturated. A better fit could thus be achieved by allowing  $C_2 < 0$ , but the resulting strain function would be non-monotonic, and show an unphysical increase at large compressive strain. We fixed  $C_2$  to zero for fitting all datasets. We also find that  $C_1 \sim 10^{-2}$ , and that  $C_1$  and  $B_{c20}$  are correlated. This can be understood, since the value of the critical field at  $\epsilon_a^*$  is  $B_{c2}(T, \epsilon_a^*) = B_{c20} [1 - (81/2)C_0^2 C_1 \epsilon_0^4]$ , up to terms of order  $(T/T_{c0})^\gamma$  and  $\epsilon_0^8$ . The value of  $B_{c2}(T, \epsilon_a^*)$  can be reproduced by fixing one of the parameters  $B_{c20}$  or  $C_1$ , and adjusting the other, without affecting significantly the  $B_{c2}(T, \epsilon_a)$  curve. We have chosen to fix  $C_1 = 0.035$ , such that the fitted value of  $B_{c20}$  is 28.6 T, as in Ref. 14. A theoretical estimate of  $C_1$  can be obtained from first-principles calculations, as described in Appendix A. The Murnaghan formula for the elastic energy is of third order in the quadratic strain invariants. It can be used to derive a fourth-order expression in the linear invariants  $I_1, J_2$ , and  $J_3$  [Eq. (A5)]. In the latter expression, the ratio between the coefficients of the  $I_1^4$  and  $I_1^2 J_2$  terms corresponds to  $C_1$ . Using the equilibrium theoretical Lamé and Murnaghan coefficients given in Appendix A, we thus obtain  $C_1 = 0.048$ . With the effective coefficients which fit the elastic energy in the strain configuration of the Furukawa dataset (see below, the discussion of Fig. 2), we find  $C_1 = 0.032$ , in excellent agreement with the value 0.035 used in the fits.

With  $C_1$  and  $C_2$  fixed to 0.035 and 0, respectively, the four adjustable parameters of the model are  $B_{c20}, \epsilon_0, \epsilon_a^*$ , and  $C_0$ .  $\epsilon_a^*$  is close to the strain at which the critical field reaches a

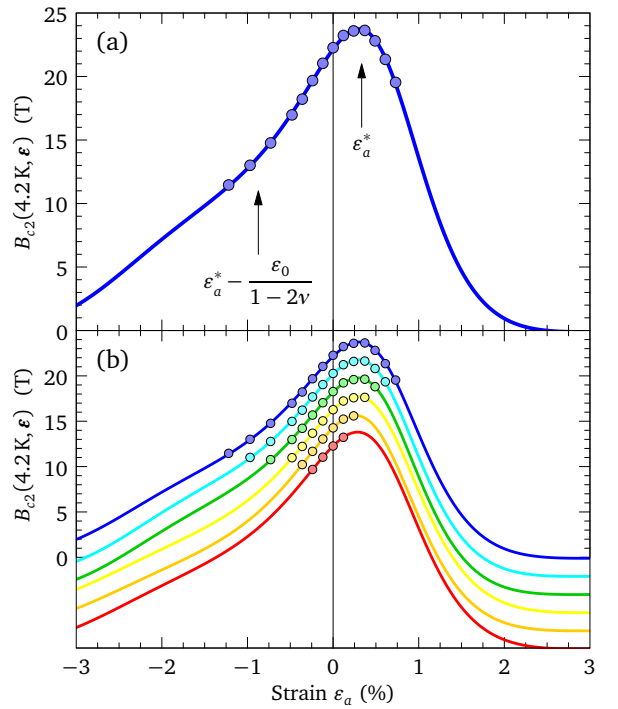


FIG. 1. Fit of the model (12) and (15), to the Furukawa dataset of Ref. 14. The following model parameters were fixed (see text):  $\alpha = 3$ ,  $\gamma = 1.5$ ,  $T = 4.2$  K,  $T_{c0} = 17$  K,  $\nu = 0.36$ ,  $\beta = 1$ ,  $C_1 = 0.035$ ,  $C_2 = 0$ . In panel (a), the whole dataset was used, and the resulting fitted parameters are  $B_{c20} = 28.6$  T,  $\epsilon_0 = 0.34\%$ ,  $\epsilon_a^* = 0.33\%$ , and  $C_0 = 1.70$ . In panel (b), subsets of the data were considered: each curve was fitted to the subset of points shown on top of it. The curves are offset vertically by 2 T for clarity.

maximum; it is therefore strongly constrained by the data, and has an immediate physical interpretation as  $-\epsilon_{10}$ , i.e., minus the longitudinal deviatoric pre-strain.  $\epsilon_0$  controls the asymmetry of the strain function with respect to  $\epsilon_a = \epsilon_a^*$ : the function is symmetric if  $\epsilon_0 = 0$ , a property also verified by the exponential strain function of Ref. 14. This shows that the asymmetry is due to the hydrostatic pre-compression of the superconductor. The measurements of Ref. 32 support this claim: more symmetric scaling curves are observed for bare wires than for jacketed wires. The asymmetry of the experimental strain function is a characteristic change to a weaker slope, appearing under tensile strain in wires which have a compressive hydrostatic pre-strain. In all datasets of Ref. 14 showing a change of slope, the latter is seen under compressive strain, suggesting that the superconductor in the strands was subjected to a tensile hydrostatic pre-strain. The strain function (15) displays a change of slope at  $\epsilon_a \approx \epsilon_a^* - \epsilon_0 / (1 - 2\nu)$ . Consistently with the experiments, the change of slope occurs on the tensile side if  $\epsilon_0 < 0$ , and on the compressive side if  $\epsilon_0 > 0$ , because  $\nu < 1/2$ .

Figure 1(a) shows a fit of the model to the Furukawa dataset of Ref. 14. The resulting positive value  $\epsilon_0 = 0.34\%$  can be understood, since the change of slope occurs on the compressive side. As expected, the cubic point  $\epsilon_a^*$  is close to where the maximum occurs. The initial longitudinal strain

TABLE II. Parameters resulting from fitting the model (12) and (15) to the datasets of Ref. 14, including strands fabricated using the bronze route (BR), the internal-tin method (IT), and the powder-in-tube method (PIT). The fixed model parameters are as in Fig. 1. The last column gives the root-mean square deviation. Note that the constants  $C_i$  refer to strain values expressed in percentages.

Strand	Type	$B_{c20}$ (T)	$\varepsilon_0$ (%)	$\varepsilon_a^*$ (%)	$C_0$	RMS (T)
Furukawa	BR	28.6	0.34	0.33	1.70	0.10
VAC	BR	28.4	0.30	0.35	1.99	0.06
OKSC	IT	28.2	0.29	0.11	2.12	0.02
OST	IT	28.8	0.40	0.14	1.40	0.07
PORI	IT	28.6	0.39	0.13	1.45	0.12
U.G.8305	BR	28.6	0.33	0.32	1.40	0.08
U.G.7567	IT	29.3	0.40	0.29	1.33	0.04
U.G.0904	PIT	31.1	0.34	0.21	1.63	0.05

$\varepsilon_{l0} = \varepsilon_0 - \varepsilon_a^*$  is almost zero, but the transverse pre-strain  $\varepsilon_{t0} = \varepsilon_0 + \nu \varepsilon_a^* = 0.46\%$  is tensile. The fitted curve is robust if fewer data points are used, as demonstrated in Fig. 1(b). The values obtained for  $\varepsilon_0$  and  $\varepsilon_a^*$ , in particular, vary by no more than  $\sim 10\%$  when data points are removed.

Similar fits can be achieved to the other datasets reported in Ref. 14. The resulting parameters are collected in Table II. In all cases, we find a positive value of  $\varepsilon_0 \sim 0.3\text{--}0.4\%$ , indicating that the superconductor in the strands was subject to a tensile hydrostatic pre-strain. The net longitudinal pre-strain  $\varepsilon_{l0}$  is close to zero for the wires prepared by following the bronze route, and positive for the others. We note that the weight factor  $w(\varepsilon)$  remains smaller than unity in all fits, as needed for the consistency of Eq. (6).

The data reported in Refs. 32 and 34 for the jacketed wires are the only ones, to our knowledge, which present a change of slope for tensile strain. This change of slope occurs at  $\varepsilon_a \sim 0.83\%$  in a wire where the largest critical current is observed at  $\varepsilon_a \sim 0.55\%$ . In these experiments, the lattice parameters were measured as a function of strain. In this particular wire, the maximum of the critical current coincides with the point  $\varepsilon_a^*$  of cubic symmetry (see Fig. 11 of Ref. 32). The measured lattice parameter at the cubic point is  $5.276 \text{ \AA}$ , while the reported equilibrium parameter is  $5.28 \text{ \AA}$ . Thus the hydrostatic pre-strain is  $\varepsilon_0 \approx -0.076\%$ . According to our model, the change of slope is expected at a strain  $-\varepsilon_0/(1-2\nu)$  measured from the position of the maximum, as indicated in Fig. 1(a), that is, at  $\varepsilon_a \sim 0.82\%$ , in very good agreement with the observations.

We now turn to the discussion of the anharmonic energy. The core idea of the model is that the strain dependence of the critical properties is governed by the anharmonic contributions to the elastic energy [Eq. (11)]. Since the parametrization (14) provides a good fit, it allows one to extract the function  $\tilde{U}(\varepsilon)$  from experimental data, in view of a comparison with an independent determination of the anharmonic energy. We have calculated the elastic energy of bulk  $\text{Nb}_3\text{Sn}$  from first-principles, in a strain configuration as determined for the Furukawa dataset in Table II (see

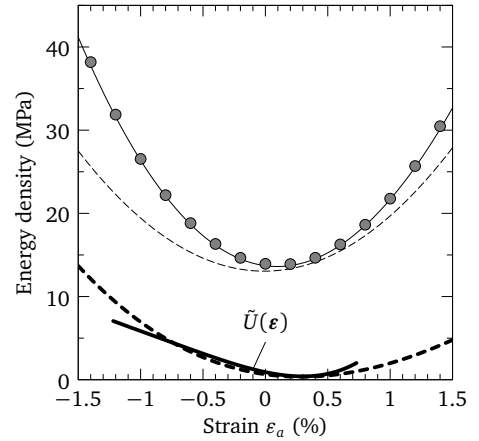


FIG. 2. Elastic and anharmonic energies of strained  $\text{Nb}_3\text{Sn}$ . The dots are the result of first-principles calculations for the strain configuration of the Furukawa dataset in Table II. The thin solid line is a fit to Eq. (A1), which contains harmonic (thin dashed) and anharmonic (thick dashed) contributions. The thick solid line is the anharmonic energy (16) for  $b = 23$  and  $\tau = 0.9$  ps, in the range of strain where experimental data is available.

Appendix A for details). The result is shown as a function of applied strain in Fig. 2. In order to extract the anharmonic terms, we fitted these data using Eq. (A1). Such a fit can not determine reliably the five elastic constants. We therefore fixed the Young modulus and Poisson ratio to the values  $E = 130$  GPa and  $\nu = 0.36$  measured on  $\text{Nb}_3\text{Sn}$  strands, and fitted the three Murnaghan coefficients  $\ell$ ,  $m$ , and  $n$ . The resulting fit is the thin solid line in Fig. 2, and yields a nonlinear factor  $b = 23$  [Eq. (A4)], and an estimate  $C_1 = 0.032$ , as indicated previously. Setting the Murnaghan coefficients to zero, we obtain the quadratic energy shown as a thin dashed line. (Notice that this function is not exactly quadratic in  $\varepsilon_a$ , due to the pre-strain.) The difference is the anharmonic energy, shown as a thick dashed line.

Using the expression of  $Q$  given near the end of Sec. II B, the relation between  $\rho v^2$  and the Young modulus and Poisson ratio (Appendix A), and setting  $C_2 = 0$ , the anharmonic energy (14) becomes

$$\tilde{U}(\varepsilon) = \frac{E}{1-2\nu} \frac{1-\nu}{1+\nu} \left( \frac{8/3}{b\omega_D\tau} \right)^2 C_0^2 (C_1 I_1^4 + I_1^2 J_2 + \delta J_2^2). \quad (16)$$

We take  $E = 130$  GPa and  $\nu = 0.36$  as above, the parameters of the Furukawa dataset, and  $\omega_D = 31$  THz, corresponding to a Debye temperature of 234 K (Ref. 35). With  $b$  fixed to the value 23 quoted above, we adjust  $\tau$  such that the order of magnitude of  $\tilde{U}(\varepsilon)$  agrees with the anharmonic energy calculated from first principles: this leads to  $\tau \sim 0.9$  ps (Fig. 2). Repeating the analysis for all datasets in Table II, we consistently find values of  $b$  of the order of 20, and values of  $\tau$  between 0.8 and 1.3 ps. These values are smaller than the thermal limit  $\hbar/(k_B T) = 11$  ps at 4.2 K. However, they are comparable to the lifetime of acoustic phonons in  $\text{Nb}_3\text{Sn}$ . In the superconducting state, the width of the acoustic phonons lines measured by inelastic neutron scattering<sup>36</sup>

is typically  $2\Gamma = 0.6\text{--}1.2$  meV. The corresponding phonon lifetime is  $\tau_{\text{ph}} = \hbar/(2\Gamma) = 0.55\text{--}1.1$  ps. We conclude that the phonon lifetime is the limiting factor in the nonlinear generation of sum and difference-frequency phonons. The nice agreement between  $\tau$  as determined from the fits and  $\tau_{\text{ph}}$  is an encouraging consistency check of our theory.

#### IV. CONCLUSION

The modifications of the superconducting properties induced by strain in  $\text{Nb}_3\text{Sn}$ , the most promising candidate for the next-generation high-power magnets, has major practical consequences. To explain this strain dependence, we have developed a theory which emphasizes the importance of anharmonicity in the deformation potential, as was put forward by Marckiewicz.<sup>13</sup> The theory is build upon the assumption that the strain-induced modifications of the superconducting properties are mainly due to a widening of the electron-phonon spectral function, which reduces the electron-phonon coupling responsible for superconductivity. This widening is attributed to the nonlinear generation of sum- and difference-frequency phonons by the anharmonic terms in the elastic energy. We have expressed the strain function, which gives the dependence of the upper critical field on strain, as a function of the anharmonic energy. This function is exponential in the strain, as recent investigations have suggested.<sup>14</sup> The theory can fit critical-field data measured on  $\text{Nb}_3\text{Sn}$  wires, and allowed us to extract the anharmonic energy from these measurements. This anharmonic energy compares favorably with first-principles calculations for strained  $\text{Nb}_3\text{Sn}$ .

The model indicates that the pre-strain state of the superconductor plays a big role in lowering the maximum critical field. Any reduction of the pre-strain is expected to produce an increase of  $B_{c2}$ . Furthermore, in the strands considered, the superconductor seems to be in a pre-strain state involving a tensile hydrostatic part of the order of 0.3–0.4%, as well as a deviatoric part. In the strands produced following the bronze route, the hydrostatic pre-strain is nearly cancelled, in the direction of the strand, by a longitudinal compressive term, while in the transverse directions the net strain is a tensile one, of the order of 0.45%. For strands produced by the internal-tin and powder-in-tube methods, the model suggests that the net pre-strain is less anisotropic, typically 0.1–0.3% (respectively, 0.3–0.5%) in the longitudinal (respectively, transverse) directions. The more isotropic pre-strain of the latter wires may explain their tendency to exhibit slightly larger critical fields. More generally, our theory suggest that any treatment or engineering step leading to a reduction of the anharmonicity, would result in an improvement of the superconducting properties under strain.

#### ACKNOWLEDGMENTS

We are grateful to C. Senatore, G. Mondonico, and T. Jarlborg for useful discussions. This work was supported by the Swiss National Science Foundation through Division II and MaNEP.

#### Appendix A: Elements of nonlinear elasticity, and theoretical elastic constants of bulk $\text{Nb}_3\text{Sn}$

The theory of nonlinear elasticity, and the propagation of waves in a nonlinear elastic medium, have been described many times. In order to fix the notations, we review here the elements of the theory which are relevant for our study. The elastic energy density of an isotropic medium, up to third order in the strain tensor  $\varepsilon_{ij}$ , can be expressed as<sup>37,38</sup>

$$U = \frac{\lambda + 2\mu}{2} I_1^2 - 2\mu I_2 + \frac{\ell + 2m}{3} I_1^3 - 2m I_1 I_2 + n I_3. \quad (\text{A1})$$

$\lambda$  and  $\mu$  are the second-order elastic constants (Lamé coefficients),  $\ell$ ,  $m$ , and  $n$  are the third-order Murnaghan coefficients, and  $I_{1,2,3}$  are three invariants of the strain tensor,  $I_1 = \varepsilon_{ii}$  (the usual index summation convention is used),  $I_2 = \varepsilon_{11}\varepsilon_{22} - \varepsilon_{12}\varepsilon_{21} + \varepsilon_{22}\varepsilon_{33} - \varepsilon_{23}\varepsilon_{32} + \varepsilon_{33}\varepsilon_{11} - \varepsilon_{31}\varepsilon_{13}$ , and  $I_3 = \det \varepsilon_{ij}$ . For a deformation represented by the displacement field  $\mathbf{u}(\mathbf{x})$ , the components of the strain tensor are

$$\varepsilon_{ij} = \frac{1}{2} \left( \frac{\partial u_i}{\partial x_j} + \frac{\partial u_j}{\partial x_i} + \frac{\partial u_k}{\partial x_i} \frac{\partial u_k}{\partial x_j} \right). \quad (\text{A2})$$

The elastic waves obey the equation of motion  $\rho \ddot{u}_i = \partial \sigma_{ij} / \partial x_j$ , where  $\rho$  is the mass density, and  $\sigma_{ij}$  is the stress tensor. Without attenuation and external driving forces, the stress tensor is  $\sigma_{ij} = \partial U / \partial (\partial u_i / \partial x_j)$ . For a longitudinal plane wave of amplitude  $A$  propagating in the direction  $x$ ,  $\mathbf{u}(\mathbf{x}, t) = \hat{\mathbf{x}} A(x, t)$ , and ignoring terms of order three and above in the displacement field, the equation of motion becomes

$$\frac{\partial^2 A}{\partial x^2} - \frac{1}{v^2} \frac{\partial^2 A}{\partial t^2} = -b \frac{\partial}{\partial x} \left( \frac{\partial A}{\partial x} \right)^2, \quad (\text{A3})$$

where the propagation velocity is given by  $\rho v^2 = \lambda + 2\mu$ , and the nonlinear factor is

$$b = \frac{3}{2} + \frac{\ell + 2m}{\lambda + 2\mu}. \quad (\text{A4})$$

We discuss in Appendix B a particular solution of Eq. (A3), which describes, starting from two initial waves, the nonlinear generation of a third wave with sum frequency.

In order to estimate the elastic coefficients of  $\text{Nb}_3\text{Sn}$ , we have performed first-principles electronic-structure calculations using QUANTUM ESPRESSO,<sup>39</sup> and ultra-soft pseudopotentials.<sup>40</sup> We used a Monkhorst-Pack mesh of  $12 \times 12 \times 12$   $k$ -points for the Brillouin-zone integrations, with a 0.002 Rydberg gaussian broadening of the levels. The wave-function cutoff was set to 40 Rydberg.

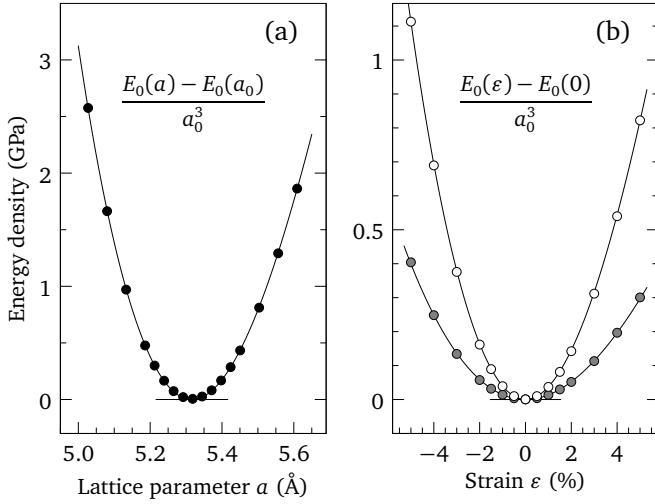


FIG. 3. Elastic energy of Nb<sub>3</sub>Sn for (a) hydrostatic strain and (b) longitudinal (gray dots) and transverse (white dots) strain. The dots are the first-principles results, the lines are fits to Eq. (A1).

The total energy of the cubic crystal is plotted in Fig. 3(a) as a function of the lattice parameter. For hydrostatic strain, i.e.,  $\varepsilon_{ij} = \delta_{ij}\varepsilon$ , the formula (A1) reduces to the simple form  $U = (9K/2)\varepsilon^2 + (9\ell + n)\varepsilon^3$ , where  $K = \lambda + 2\mu/3$  is the bulk modulus. This form, with  $\varepsilon = a/a_0 - 1$ , can fit the data in Fig. 3(a) very well, and yields an equilibrium lattice parameter  $a_0 = 5.32$  Å, a bulk modulus  $K = 165$  GPa, and the relation  $9\ell + n = -2368$  GPa. As Nb<sub>3</sub>Sn is not isotropic, these coefficients should be regarded as effective parameters used to represent the elastic energy of the material. The theoretical lattice parameter is 0.8% larger than the low-temperature experimental value of 5.28 Å reported in Ref. 32. The theoretical bulk modulus compares very well with the experimental value of 163 GPa reported in Ref. 41. In order to determine the remaining coefficients, we have calculated the energy for two non-hydrostatic diagonal strains, either longitudinal ( $\varepsilon_{11} = \varepsilon$ ,  $\varepsilon_{22} = \varepsilon_{33} = 0$ ) or transverse ( $\varepsilon_{11} = 0$ ,  $\varepsilon_{22} = \varepsilon_{33} = \varepsilon$ ). The results of the calculation and the fits are shown in Fig. 3(b). In the longitudinal case, the elastic energy (A1) is  $U = (3K/2)(1 - \nu)/(1 + \nu)\varepsilon^2 + (1/3)(\ell + 2m)\varepsilon^3$ , where  $\nu = (\lambda/2)/(\lambda + \mu)$  is the Poisson ratio, while in the transverse case we have  $U = 3K/(1 + \nu)\varepsilon^2 + (4/3)(2\ell + m)\varepsilon^3$ . Using the value of  $K$  obtained above, the fits yield  $\nu = 0.28$ ,  $\ell + 2m = -1232$  GPa, and  $2\ell + m = -874$  GPa. The resulting Murnaghan coefficients are therefore  $\ell = -172$ ,  $m = -530$ , and  $n = -820$  GPa.

The theoretical coefficients correspond to a Young modulus  $E = 3K(1 - 2\nu) = 218$  GPa, significantly larger than the value  $\sim 130$  GPa measured for Nb<sub>3</sub>Sn wires. The theoretical Poisson ratio is also appreciably lower than the experimental value of 0.36. These numbers can not be directly compared, however, because the experiments are performed on wires in which the Nb<sub>3</sub>Sn material is strained, in addition to being mixed with other materials forming the structure. In order to clarify the role of the pre-strain on the elastic properties

of Nb<sub>3</sub>Sn, we have calculated the elastic energy in the strain configuration considered in Sec. III A, i.e.,  $\varepsilon_{11} = \varepsilon_0 - \varepsilon_a^* + \varepsilon_a$ ,  $\varepsilon_{22} = \varepsilon_{33} = \varepsilon_0 + \nu\varepsilon_a^* - \nu\varepsilon_a$ . We used the values  $\varepsilon_0 = 0.34\%$ ,  $\varepsilon_a^* = 0.33\%$  (see Table II) and the experimental Poisson ratio  $\nu = 0.36$ . The resulting elastic energy (Fig. 2) is not well described by Eq. (A1), if the equilibrium elastic constants are used, but can be well fitted using effective parameters corresponding to the experimental values (see Sec. III B).

We close this appendix with the expression of the elastic energy (A1) in terms of the invariants  $I_1$ ,  $J_2$ , and  $J_3$  introduced in Sec. III A. These invariants are functions of the infinitesimal strains  $\varepsilon_i = \partial u_i / \partial x_i$  along the principal axes, which are related to the diagonal strains  $\varepsilon_{ii}$  by  $\varepsilon_{ii} = \varepsilon_i + \varepsilon_i^2/2$ . Inserting this in Eq. (A1), a sixth-order development in the infinitesimal strains results, which we express up to fourth order by means of the invariants  $I_1$ ,  $J_2$ , and  $J_3$ :

$$U = \frac{3\lambda + 2\mu}{6} I_1^2 + 2\mu J_2 + \frac{9\lambda + 6\mu + 18\ell + 2n}{54} I_1^3 + \frac{3\lambda + 6\mu + 6m - n}{3} I_1 J_2 + (3\mu + n) J_3 + \frac{3\lambda + 2\mu + 36\ell + 4n}{216} I_1^4 + \frac{\lambda + 2\mu + 6\ell + 10m - n}{6} I_1^2 J_2 + \frac{2\mu + 6m + n}{2} I_1 J_3 + \frac{\lambda + \mu + 4m}{2} J_2^2. \quad (\text{A5})$$

With the relations  $\lambda = E\nu/[(1 + \nu)(1 - 2\nu)]$  and  $\mu = (E/2)/(1 + \nu)$ , the second-order terms of (A5) reduce to Eq. (13).

## Appendix B: Nonlinear generation of acoustic waves

A longitudinal plane wave propagating without attenuation in an isotropic elastic solid obeys, to lowest order in the nonlinearity, the equation of motion (A3).  $A(x, t)$  is the displacement amplitude in the direction  $x$ , which is also the direction of propagation, and  $v$  is the propagation velocity. The nonlinear term in the wave equation gives rise to sum- and difference-frequency generation. We shall only consider the case of sum frequency for simplicity. In this process, two plane waves of amplitudes  $A_1(t)$  and  $A_2(t)$ , and frequencies  $\omega_1$  and  $\omega_2$ , generate a third wave of amplitude  $A_3(t)$  and frequency  $\omega_3 = \omega_1 + \omega_2$ . We assume a linear dispersion relation,  $\omega = vq$ , which means that the phase-matching condition is satisfied if the generated wave has wave number  $q_3 = q_1 + q_2$ . We therefore consider a solution of Eq. (A3) in the form

$$A(x, t) = \frac{1}{2} \left[ A_1(t)e^{iq_1(x-vt)} + A_2(t)e^{iq_2(x-vt)} + A_3(t)e^{i(q_1+q_2)(x-vt)} + \text{c.c.} \right]. \quad (\text{B1})$$

The amplitudes  $A_i(t)$  are slow functions of  $t$ , and the initial condition is  $A_3(0) = 0$ . Inserting the solution (B1) into the wave equation (A3), and neglecting terms of order  $d^2 A_i(t)/dt^2$ , we obtain the evolution of the amplitude for



each of the three frequencies:

$$dA_1(t)/dt = -(bv/2)q_2q_3A_2^*(t)A_3(t) \quad (\text{B2a})$$

$$dA_2(t)/dt = -(bv/2)q_1q_3A_1^*(t)A_3(t) \quad (\text{B2b})$$

$$dA_3(t)/dt = +(bv/2)q_1q_2A_1(t)A_2(t). \quad (\text{B2c})$$

Taking the time derivative of (B2c), and using (B2a) and (B2b), the following second-order equation results for  $A_3(t)$ :

$$d^2A_3(t)/dt^2 = -(b/2)^2\omega_1\omega_2 \times [q_1q_3|A_1(t)|^2 + q_2q_3|A_2(t)|^2]A_3(t). \quad (\text{B3})$$

In order to eliminate the amplitudes  $A_1(t)$  and  $A_2(t)$  from this equation, we note that the quantity

$$C = q_1q_3|A_1(t)|^2 + q_2q_3|A_2(t)|^2 + 2q_3^2|A_3(t)|^2 \quad (\text{B4})$$

is conserved during the evolution governed by (B2). This allows us to rewrite Eq. (B3) as a differential equation for  $A_3(t)$  only:

$$\frac{d^2A_3(t)}{dt^2} = -(b/2)^2\omega_1\omega_2 (C - 2q_3^2|A_3(t)|^2)A_3(t). \quad (\text{B5})$$

This nonlinear equation admits a remarkably simple solution, which satisfies the initial condition  $A_3(0) = 0$ , namely

$$A_3(t) = \frac{1}{q_3} \sqrt{\frac{C}{2}} \tanh \left( t \sqrt{\frac{C}{2}} (b/2)^2 \omega_1 \omega_2 \right). \quad (\text{B6})$$

The generated amplitude increases first linearly with time, and then saturates. The saturation amplitude is reached when the energy available in the two primary waves has been completely transferred to the secondary wave. We therefore identify the energy carried by the generated wave, when it reaches saturation, with the anharmonic energy,  $\tilde{U}$ , that was initially available for sum-frequency generation. Since the energy density of an harmonic wave of frequency  $\omega$  and amplitude  $A$  is  $\rho(\omega A)^2$ , we obtain an interpretation for the conserved quantity  $C$ , in terms of  $\tilde{U}$ :

$$\tilde{U} = \rho[\omega_3 A_3(\infty)]^2 = \rho v^2 (C/2). \quad (\text{B7})$$

This allows us to write the amplitude of the generated wave in the form quoted in the main text,

$$\omega_3 A_3(t) = \sqrt{\tilde{U}/\rho} \tanh \left( t q_{12} \sqrt{\tilde{U}/\rho} \right), \quad (\text{B8})$$

where  $q_{12} = |b/2| \sqrt{q_1 q_2}$ .

- 
- <sup>1</sup> T. Miyazaki, Y. Murakami, T. Hase, M. Shimada, K. Itoh, T. Kiyoshi, T. Takeuchi, K. Inoue, and H. Wada, *IEEE Trans. Appl. Supercond.* **9**, 2505 (1999).
- <sup>2</sup> N. Mitchell, P. Bauer, D. Bessette, A. Devred, R. Gallix, C. Jong, J. Knaster, P. Libeyre, B. Lim, A. Sahu, and F. Simon, *Fusion Engineering and Design* **84**, 113 (2009).
- <sup>3</sup> L. Bottura, G. de Rijk, L. Rossi, and E. Todesco, *IEEE Trans. Appl. Supercond.* **22**, 4002008 (2012).
- <sup>4</sup> G. Arbman and T. Jarlborg, *Sol. State Com.* **26**, 857 (1978).
- <sup>5</sup> B. M. Klein, L. L. Boyer, and D. A. Papaconstantopoulos, *Phys. Rev. Lett.* **42**, 530 (1979).
- <sup>6</sup> See, e.g., C. Paduani, *Sol. State Com.* **149**, 1269 (2009).
- <sup>7</sup> L. P. Gor'kov and O. N. Dorokhov, *J. Low Temp. Phys.* **22**, 1 (1976).
- <sup>8</sup> J. W. Ekin, *Cryogenics* **20**, 611 (1980).
- <sup>9</sup> D. M. J. Taylor and D. P. Hampshire, *Supercond. Sci. Technol.* **18**, S241 (2005).
- <sup>10</sup> B. ten Haken, A. Godeke, and H. H. J. ten Kate, *J. App. Phys.* **85**, 3247 (1999).
- <sup>11</sup> A. Godeke, *Performance boundaries in Nb<sub>3</sub>Sn superconductors*, Ph.D. thesis, University of Twente, Enschede, The Netherlands (2005).
- <sup>12</sup> L. R. Testardi, *Phys. Rev. B* **3**, 95 (1971).
- <sup>13</sup> W. D. Markiewicz, *Cryogenics* **44**, 767 (2004).
- <sup>14</sup> B. Bordini, P. Alknes, L. Bottura, L. Rossi, and D. Valentini, *Supercond. Sci. Technol.* **26**, 075014 (2013).
- <sup>15</sup> D. F. Valentini, *Anharmonic model of the strain sensitivity of low temperature superconductors*, Master's thesis, Polytechnic of Milan, Milano (2012).
- <sup>16</sup> B. Bordini, L. Bottura, G. Mondonico, L. Oberli, D. Richter, B. Seeber, C. Senatore, E. Takala, and D. Valentini, *IEEE Trans. Appl. Supercond.* **22**, 6000304 (2012).
- <sup>17</sup> D. J. Scalapino, J. R. Schrieffer, and J. W. Wilkins, *Phys. Rev.* **148**, 263 (1966).
- <sup>18</sup> W. L. McMillan, *Phys. Rev.* **167**, 331 (1968).
- <sup>19</sup> R. C. Dynes, *Sol. State Com.* **10**, 615 (1972).
- <sup>20</sup> P. B. Allen and R. C. Dynes, *Phys. Rev. B* **12**, 905 (1975).
- <sup>21</sup> P. Morel and P. W. Anderson, *Phys. Rev.* **125**, 1263 (1962).
- <sup>22</sup> G. De Marzi, L. Morici, L. Muzzi, A. della Corte, and M. Buon-giorno Nardelli, *J. Phys.: Cond. Mat.* **25**, 135702 (2013).
- <sup>23</sup> S. Oh and K. Kim, *J. App. Phys.* **99**, 033909 (2006).
- <sup>24</sup> A. Godeke, *Supercond. Sci. Technol.* **19**, R68 (2006).
- <sup>25</sup> E. L. Wolf, J. Zasadzinski, G. B. Arnold, D. F. Moore, J. M. Rowell, and M. R. Beasley, *Phys. Rev. B* **22**, 1214 (1980).
- <sup>26</sup> J. Kwo and T. H. Geballe, *Phys. Rev. B* **23**, 3230 (1981).
- <sup>27</sup> K. E. Kihlstrom, D. Mael, and T. H. Geballe, *Phys. Rev. B* **29**, 150 (1984).
- <sup>28</sup> O. Delaire, M. S. Lucas, J. A. Muñoz, M. Kresch, and B. Fultz, *Phys. Rev. Lett.* **101**, 105504 (2008).
- <sup>29</sup> R. W. Boyd, *Nonlinear Optics*, 3rd ed. (Academic Press, Waltham, 2003).
- <sup>30</sup> P. G. de Gennes, *Superconductivity of metals and alloys*, Advanced book classics (Perseus, Cambridge, 1999).
- <sup>31</sup> B. ten Haken, *Strain effects on the critical properties of high-field superconductors*, Ph.D. thesis, University of Twente, Enschede, The Netherlands (1994).
- <sup>32</sup> L. Muzzi, V. Corato, A. della Corte, G. De Marzi, T. Spina, J. Daniels, M. Di Michiel, F. Buta, G. Mondonico, B. Seeber, R. Flükiger, and C. Senatore, *Supercond. Sci. Technol.* **25**, 054006 (2012).
- <sup>33</sup> J. K. Freericks, A. Y. Liu, A. Quandt, and J. Geerk, *Phys. Rev. B* **65**, 224510 (2002).
- <sup>34</sup> G. Mondonico, B. Seeber, C. Senatore, R. Flükiger, V. Corato, G. D. Marzi, and L. Muzzi, *J. App. Phys.* **108**, 093906 (2010).

- <sup>35</sup> V. Guritanu, W. Goldacker, F. Bouquet, Y. Wang, R. Lortz, G. Goll, and A. Junod, *Phys. Rev. B* **70**, 184526 (2004).
- <sup>36</sup> J. D. Axe and G. Shirane, *Phys. Rev. B* **8**, 1965 (1973).
- <sup>37</sup> L. D. Landau and E. M. Lifshitz, *Theory of Elasticity*, 3rd ed. (Elsevier, Oxford, 1986).
- <sup>38</sup> F. D. Murnaghan, *Finite Deformation of an Elastic Solid* (John Wiley & Sons, New York, 1951).
- <sup>39</sup> P. Giannozzi *et al.*, *J. Phys.: Cond. Mat.* **21**, 395502 (2009).
- <sup>40</sup> The pseudo-potential files are Nb.pw91-nsp-van.UPF and Sn.pw91-n-van.UPF from [www.quantum-espresso.org](http://www.quantum-espresso.org).
- <sup>41</sup> L. R. Testardi, *Phys. Acoust.* **10**, 193 (1973).